Journal of Sound and Vibration (1998) **217**(4), 619–636
Article No. sv981811

THE IMPEDANCE OF PERFORATED PLATES SUBJECTED TO GRAZING GAS FLOW AND BACKED BY POROUS MEDIA†

R. KIRBY AND A. CUMMINGS

Department of Engineering Design and Manufacture, *University of Hull*, *Hull HU*6 7*RX*, *England*

(*Received* 13 *March* 1998)

Experimental data of the acoustic impedance of multiply perforated plates exposed to fully developed grazing gas flow in a duct, both with and without a backing layer of porous material, are presented. Both circular perforations and "louvres" are included in the investigation. Empirical formulae are presented for the impedance of plates with no porous backing layer, in terms of dimensionless parameters, and an heuristic method of including the effects of the porous medium is described. It is observed that the porous backing layer has a large effect on the impedance of plates with circular perforations, and little or no effect on louvred perforates.

1. INTRODUCTION

The use of perforated plates and tubes is common in applications such as vehicle exhaust silencers, attenuators in air moving ducts and duct linings in jet engines. The perforates are usually exposed to the mean gas flow, and it is known that this has an effect on the acoustic performance of the silencer. In exhaust silencers, perforates are used in both reactive and dissipative elements. In dissipative silencers, which are of particular interest here, the perforate commonly takes the form of a concentric tube which is surrounded by a porous sound absorbing material contained in a box, and prevents loss of or damage to the material while still being permeable to sound. In most cases the perforate is subjected to a grazing gas flow. An understanding of the acoustic behaviour of perforates under such conditions is necessary for the formulation of accurate methods of dissipative silencer modelling. Investigations of the effects of grazing flow have so far been confined to perforates in the absence of porous media. Although in dissipative silencers it is common for a porous material to be situated adjacent to one side of the perforate, the influence that this perforate has on the overall acoustic characteristics of a silencer has received very little attention in the literature.

†A shorter version of this paper was presented at the Inter-Noise 96 conference in Liverpool, 30 July–2 August 1996.

0022–460X/98/440619 + 18 $30.00/0

Indeed it is common in most dissipative silencer models to ignore the acoustic influence of the perforate altogether. It will be reported in this paper that, especially when both a grazing flow and a porous material are present, the acoustic impedance of perforates cannot be ignored in silencer design, and that this applies even to perforates with a high percentage open area.

The mechanisms that lie behind the acoustic behaviour of perforates with grazing gas flow are still not fully understood. It is well established that the presence of mean flow (grazing or normal) increases the resistance and decreases the mass end correction as compared to the zero flow situation (see for example the experimental data of reference [1]). The mechanisms behind this observation have been the subject of considerable debate. In an effort to investigate the physical reasons behind the change in impedance, flow visualization techniques and hot-film and laser anenometry have been used by a number of authors in order to observe the flow patterns close to the orifice (see for example references [2, 3]). Investigations have been concentrated on describing how sound energy is dissipated in the near field of the orifice and theoretical models have been developed, although in order to make the models tractable the problem has generally been oversimplified. For example, Howe [4]—in a theoretical investigation of a two-dimensional slot—proposed a model based upon vortex shedding from the upstream lip of the orifice but omitted the effects of mean shear in the slot, which may be of importance at higher flow speeds. Walker and Charwat [5] included the effect of the free shear layer by formulating a ''hinged-lid'' model to account for the influx and efflux of the free shear layer at the downstream edge of the orifice. Their model is strongly dependent upon where the approaching boundary layer separates, and the influence of vorticity transport was suppressed in the model. Various other theoretical models have been devised, generally based upon the behaviour of the free shear layer (see, for example, references [6–8]), but only qualitative agreement with experimental data has been reported in all cases.

The difficulties associated with theoretically modelling the acoustic behaviour of perforates subjected to grazing flow have resulted in a reliance upon experimental data. Measurement of the impedance of perforated plates has generally been restricted to single orifices, and it has been assumed that the results could be extrapolated to multi-orifice perforated plates *via* the percentage open area (or porosity) of the perforate. Ronneberger [1] measured the acoustic impedance of a single orifice under grazing flow and related the acoustic impedance to the reciprocal Strouhal number based upon the mean flow velocity U_o, orifice radius a and the radian frequency ω. In these experiments, however, the boundary layer was very thin; similar measurements under a thin boundary layer were also performed by Narayana Rao and Munjal [9]. It became apparent in later work (see reference [10]) that the boundary layer thickness affects the impedance of the orifice; this is particularly important in the study of exhaust silencers where, in most cases, fully developed turbulent flow is present. Consequently a method for quantifying the boundary layer thickness became necessary. Goldman and Panton [10] measured the boundary layer thickness close to an orifice and showed that in their particular study a ''young'' turbulent

boundary layer was present. They proposed using the friction velocity u_* to characterize the boundary layer. The friction velocity is a measure of the properties of the inner boundary layer (see reference [11]), and was used by Goldman and Panton to replace the free stream velocity in the Strouhal number. Goldman and Chung [12] confirmed that the orifice impedance was affected only by the inner region of the boundary layer and concluded that the use of the friction velocity in the Strouhal number was correct. Kooi and Sarin [13], who also measured the friction velocity, re-defined the parameters used for the resistance and mass end correction. They wrote the resistance as a function of the inverse Strouhal number u_*/fd (where f is frequency and d the orifice diameter) and the mass end correction as a function of u_*/ft (where t is the orifice depth). By carrying out tests on a range of different plates with a young turbulent boundary layer, Kooi and Sarin found that the resistance could also be written as a function of t/d and they were able to derive simple algebraic expressions for both the resistance and mass end correction. Cummings [14], who also investigated perforates with a range of t/d values but for fully developed turbulent pipe flow, found similar expressions though with slightly different forms. He found systematic differences between his results and those of Kooi and Sarin [13], and attributed this to the differing boundary layer conditions between his tests and those of Kooi and Sarin. Cummings concluded that boundary layer turbulence is an important parameter in the measurement of perforate impedance and it is necessary to measure perforates under conditions similar to those in which they are to be used. The experimental method used by Cummings [14] appears to be best suited to the present investigation; it must be assumed that any interaction between holes (see references [15, 16]) will be properly accounted for in the use of this method.

A notable deficiency in the literature on perforates subjected to grazing flow is that, to the best of the authors' knowledge, the effect of a porous material backing the perforate has not been measured. The only published work to be found involving combinations of perforates and porous media is concerned with reacting absorbers with no mean flow, for example the investigations of Ingard and Bolt [17] and Davern [18]. This is surprising considering the widespread use of porous materials in exhaust silencers.

The aim of the present investigation was to examine, experimentally, the effect of grazing gas flow on the impedance of a perforated plate backed by a porous medium for a range of parameters. To establish the additional influence of the porous material upon the impedance of the perforate, measurements are reported both with and without its presence. In addition to accounting for the extra effect of the porous medium, these measurements form the basis of a new semi-empirical model accounting for the influence of the porous material in determining the impedance of the perforate. Two types of plate perforation, both in common use in vehicle exhaust silencers, were studied in these tests: plain, circular holes and louvred holes. These cover the great majority of practical situations.

2. EXPERIMENTAL METHOD

The experimental arrangement used by Cummings [14] is appropriate here for measurements both with and without absorbing material. It is shown in

Figure 1. A square section pipe was used to carry the airflow from a variable speed air supply to the test section of the duct. The air supply was silenced by means of a large dissipative silencer close to its outlet. A square pipe was used in order to allow small test samples of perforate to be mounted easily into the wall. This

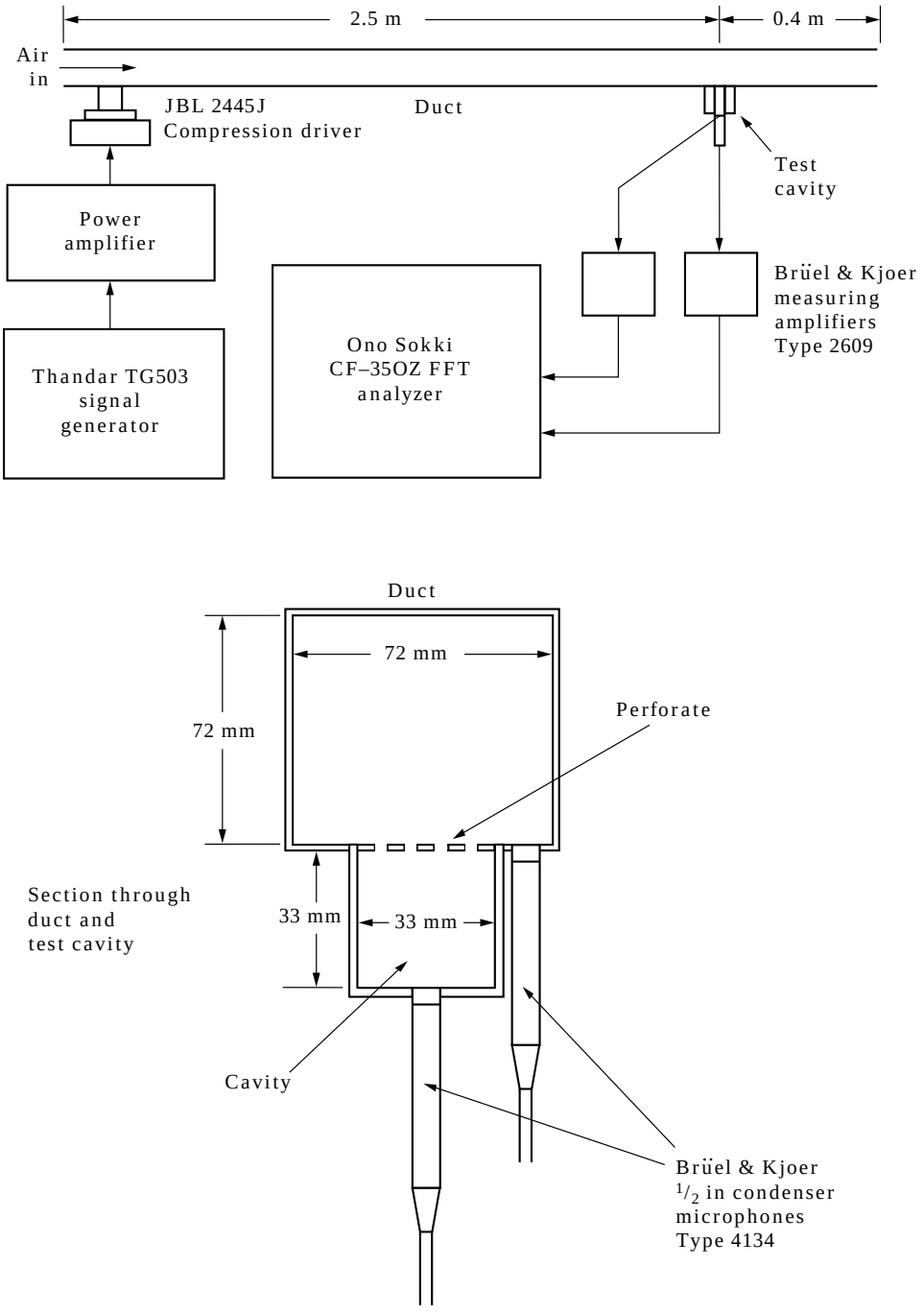

Figure 1. Apparatus for the measurement of the acoustic impedance of a perforate.

would not cause a significant departure from conditions encountered in a circular pipe provided the perforate were located away from the very corners of the pipe. To allow a turbulent boundary layer to develop, the perforate was located approximately 2·5 m from the outlet of the air supply. A sinusoidal signal, fed *via* a power amplifier to a loudspeaker mounted near to the air supply outlet, was used to generate the superimposed sound field. The perforate, once it had been mounted flush with the inner surface of the pipe, was backed by a small cavity. Depending upon the tests performed, the cavity was either filled with porous material or left empty.

The impedance measurements carried out on the perforates were based upon the two-microphone method used by both Kooi and Sarin [13] and Cummings [14]. This required sound pressure data to be taken from one microphone located in the base of the cavity and one situated in the test duct upstream of, but close to, the perforate, located flush with the wall. The two microphones together with the measuring amplifiers were phase matched to within 0·5° over the frequency range of interest, approximately from 70 Hz to 1 kHz. The "perforate impedance" or "orifice impedance" (these terms being used here interchangeably) is defined as the sound pressure differential across the perforate, divided by the particle velocity in an orifice. To determine the acoustic impedance of the perforate, measurement of the ratio of sound pressures between the two microphones was necessary, and this was performed at discrete frequencies by using an FFT analyser. If the sound pressure at the microphone in the pipe is denoted p_1 and that in the cavity p_2, then the sound pressure ratio p_2/p_1 can be written in the form

$$p_2/p_1 = R\,\mathrm{e}^{i\phi}. \tag{1}$$

If the cross-sectional areas of the orifice and cavity are, respectively, A_o and A_c (A_o being the total area of all orifices in the test sample), and if $k = \omega/c$ (c being the sound speed), then it may be shown that the impedance of the orifice, z_o, when no porous material is present, is given by

$$z_o = \rho c(A_o/A_c)[-\sin\phi + \mathrm{i}(R\cos kL - \cos\phi)]/R\sin kL, \tag{2}$$

where ρ is the mean fluid density and L is the depth of the cavity. It is convenient here to write the perforate impedance in the form

$$z_o = r_o + \mathrm{i}\omega\rho\ell, \tag{3}$$

where r_o is the resistance and ℓ is the effective orifice length, and so

$$r_o = -\rho c A_o \sin\phi/A_c R\sin kL \tag{4}$$

and

$$\ell = A_o(R\cos kL - \cos\phi)/A_c kR\sin kL. \tag{5}$$

The total orifice end correction (both sides) is found by subtracting the geometrical orifice length t from the effective length ℓ. If a porous material is present in the cavity then ρc is replaced by z_a and k by $-\mathrm{i}\Gamma$ in equations (4) and (5), where z_a is the characteristic impedance of the material and Γ the propagation constant (equal to $\mathrm{i}k_a$, k_a being the complex wavenumber in the absorbent).

The introduction of mean flow parameters is accommodated here by use of the friction velocity (see section 1). This can be written in terms of the wall shear stress τ_w [19] as $u_* = \sqrt{\tau_w/\rho}$. It was measured here by use of a Preston tube [20]. The method involves measuring the skin friction directly by placing a circular Pitot-static tube along the pipe wall, facing the flow. In calibrating a number of different Pitot-static tubes, Patel proposed the relationship

$$x^* = y^* + 2\log_{10}(1{\cdot}95y^* + 4{\cdot}1), \tag{6}$$

where $x^* = \log_{10}(\Delta p d_p^2/4\rho v^2)$ and $y^* = \log_{10}(\tau_w d_p^2/4\rho v^2)$, for $5{\cdot}6 < x^* < 7{\cdot}6$. Here, Δp is the measured difference between the stagnation and static pressures, d_p is the outside diameter of the Pitot-static tube (a Pitot-static tube 3 mm in diameter was used here) and v is the fluid kinematic viscosity. Equation (6) can be solved to give τ_w and hence u_* at any position on the wall of the pipe. Wall shear stress data measured by using the Preston tube method proved to be similar—to within engineering accuracy—to those predicted from published data of friction factor and wall shear stress distribution, as in the study of Cummings [14].

3. EXPERIMENTAL RESULTS

As mentioned in section 1, perforates with both circular and louvred holes were studied here. The circularly perforated samples will be referred to here simply as "plates" and numbered 1 to 3; the louvred perforates are also numbered 1 to 3 and referred to as "louvres". Each perforate was chosen to have a different t/d ratio. The geometry of a typical louvred hole is shown in Figure 2. The equivalent hole diameter is that of a circle having the same area as that presented by the louvred hole to the test duct. The dimensions and porosity (fractional open area) of each perforate are given in Tables 1 and 2.

3.1. ACOUSTIC IMPEDANCE WITHOUT A POROUS BACKING

Initially, the acoustic impedances of the perforates were measured without a porous material in the cavity in order both to compare the present results to those of other authors and to provide the basis for a semi-empirical model accounting for the presence of a porous material. The experimental data of acoustic impedance are presented here in the format used by Cummings [14]. This involves non-dimensionalizing both the resistance and the mass end correction, such that the normalized acoustic impedance ζ is given by

$$\zeta = z_o/\rho c = r_o/\rho c + \mathrm{i}k\ell = \theta + \mathrm{i}\chi. \tag{7}$$

Equation (2) allows θ and χ to be written as

$$\theta = -A_o \sin\phi/A_c R \sin kL \tag{8}$$

and

$$\chi = A_o(R\cos kL - \cos\phi)/A_c R \sin kL. \tag{9}$$

The resistance of the orifice, θ, has two components: the resistance induced by the flow, θ_f, and the resistance attributable to the viscous acoustic boundary layer on

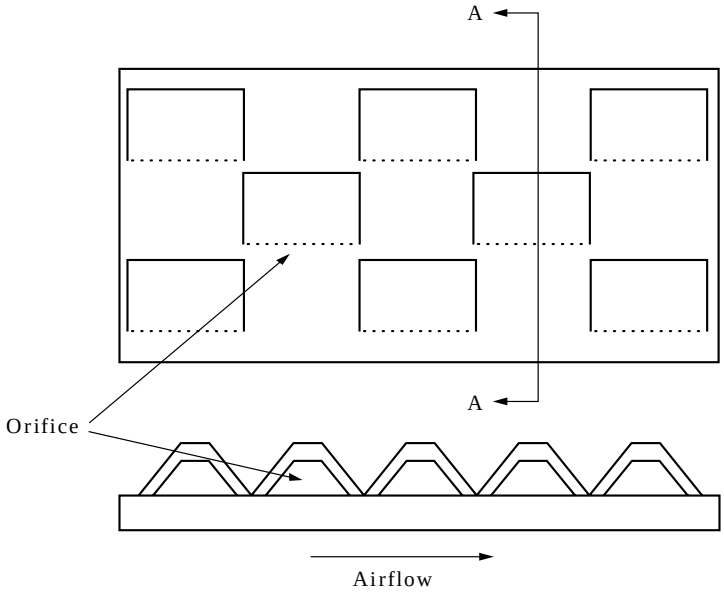

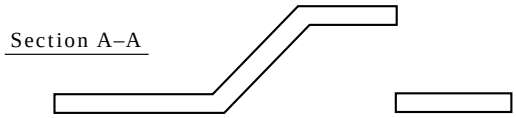

Figure 2. Geometry of a louvred hole.

TABLE 1

Dimensions of circularly perforated plates

Plate	t (mm)	d (mm)	t/d	Porosity
1	1·5	3·1	0·484	0·210
2	1·5	2·8	0·536	0·205
3	1	3·5	0·286	0·272

TABLE 2

Dimensions of louvred plates

Louvre	t (mm)	d_{equiv} (mm)	t/d	Porosity
1	1	2·25	0·444	0·04
2	1	2·92	0·342	0·09
3	1	2·73	0·366	0·08

the solid surface, θ_{visc}, where $\theta = \theta_f + \theta_{visc}$. Now $\theta_{visc} = (t/cd)\sqrt{16\pi v\ell}$ [13], and so the flow induced resistance of the orifice is given by

$$\theta_f = -A_o \sin\phi / A_c R \sin kL - (t/cd)\sqrt{16\pi v\ell}. \tag{10}$$

For the total mass end correction δ, the orifice length t is subtracted from the effective orifice length ℓ, to give

$$\delta = \ell - t, \tag{11}$$

where $\ell = \chi/k$.

The flow induced resistance is non-dimensionalized here in the form $\theta_f c/fd$ and the mass end correction is expressed as δ/δ_0 (see also reference [14]), where δ_0 is the mass end correction without flow. This is approximately equal to $0{\cdot}85d$ for an isolated orifice if $d \ll \lambda$, λ being the wavelength; in the case of louvred holes, the reference end correction δ_0 was put equal to that for a circular hole of the equivalent diameter, and so this would not be an accurate representation of the *actual* end correction. The resistance data are expressed as a function of u_*/fd and the mass end correction as a function of u_*/ft.

Measurements of the acoustic impedance of the perforates were carried out for four different friction velocities: 0·476, 0·986, 1·626 and 2·192 m/s. Measurement of the mean flow velocity profile in the boundary layer indicated that the mean flow was almost fully developed. The turbulent velocity components were not measured, but the length and width of the pipe leading from the air supply to the test section were such that the turbulence structure would be fairly representative of that encountered in typical exhaust silencer applications.

To correlate the experimental data, the curve fitting method of Cummings [14] was tried. This involves collapsing the data obtained for individual perforates into a separate pair of algebraic expressions for the resistance and the mass end correction. Cummings used this method exclusively for flat plates, and it will be shown later that the method cannot be applied to louvres. The experimental results for plates 1 to 3 are shown in Figures 3(a–d) and 4(a, b); also shown are curves from the algebraic data fitting formulae obtained by using the method of Cummings [14]. For the three flat perforates examined here the resistance curve is given by

$$\frac{\theta_f c}{fd} = \left\{26{\cdot}16\left(\frac{t}{d}\right)^{-0{\cdot}169} - 20\right\}\frac{u_*}{fd} - 4{\cdot}055, \tag{12}$$

and the mass end correction by

$$\begin{gathered}\delta/\delta_0 = 1, \qquad u_*/ft \leqslant 0{\cdot}18d/t,\\ \delta/\delta_0 = (1 + 0{\cdot}6t/d)\exp\{-(u_*/ft - 0{\cdot}18d/t)/(1{\cdot}8 + t/d)\} - 0{\cdot}6t/d,\\ u_*/ft > 0{\cdot}18d/t.\end{gathered} \tag{13}$$

The experimental results for the louvres are shown in Figures 4(c, d) and 5(a–d). Unfortunately each louvre requires a different curve fitting formula because it was found to be impossible to derive a universal empirical formula that contained both

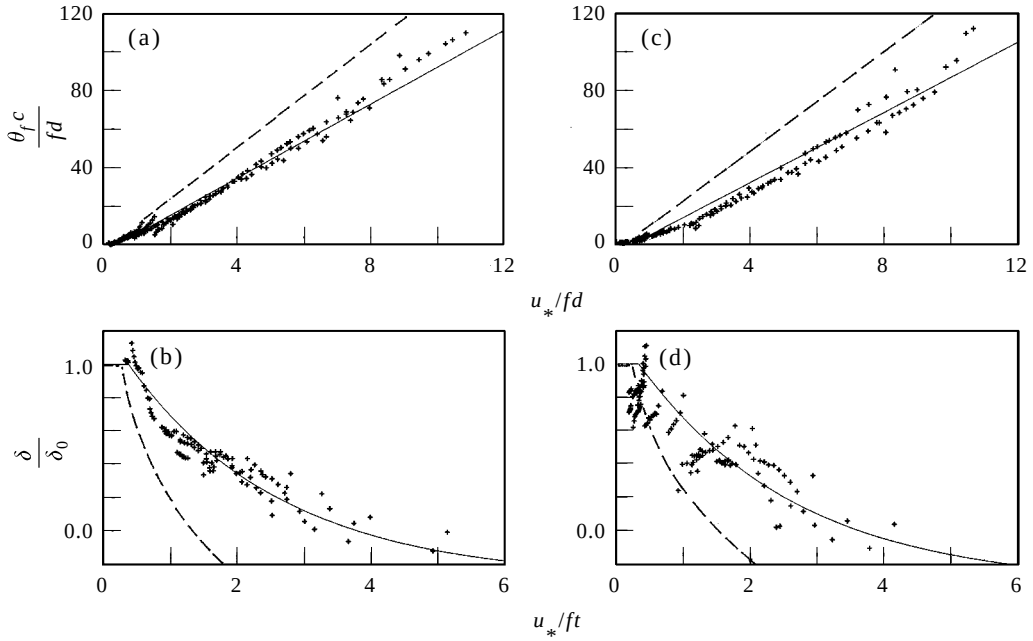

Figure 3. Acoustic impedance of plates 1 and 2. +, experiment; ——, present curve fitting formulae; ––, curve fitting formulae of Cummings [14]. Plate 1: (a) resistance, (b) end correction. Plate 2: (c) resistance, (d) end correction.

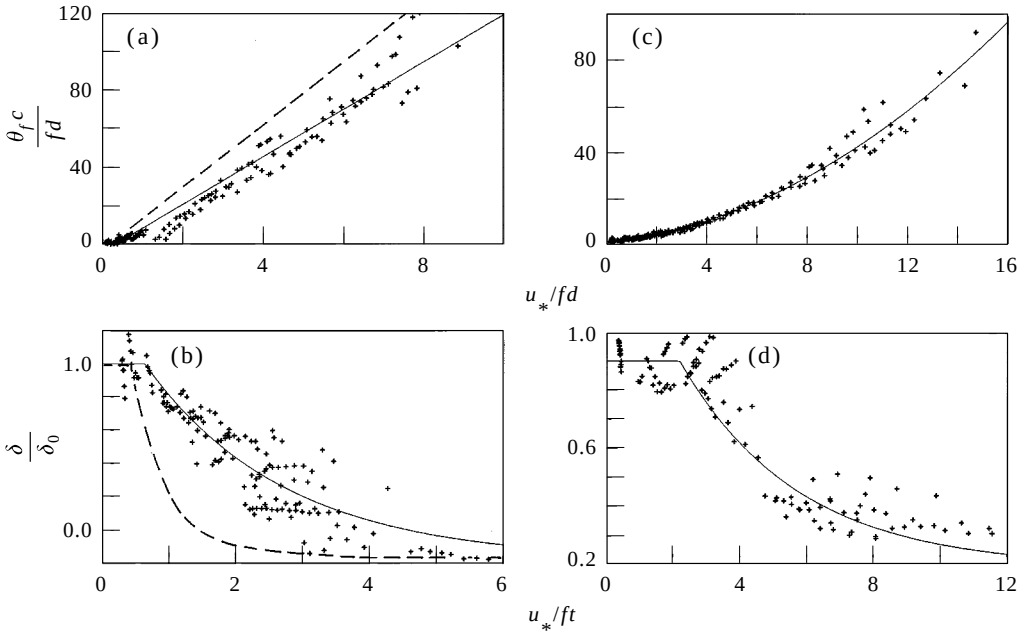

Figure 4. Acoustic impedance of plate 3 and louvre 1. +, experiment; ——, present curve fitting formulae; ––, curve fitting formulae of Cummings [14]. Plate 3: (a) resistance, (b) end correction. Louvre 1: (c) resistance, (d) end correction.

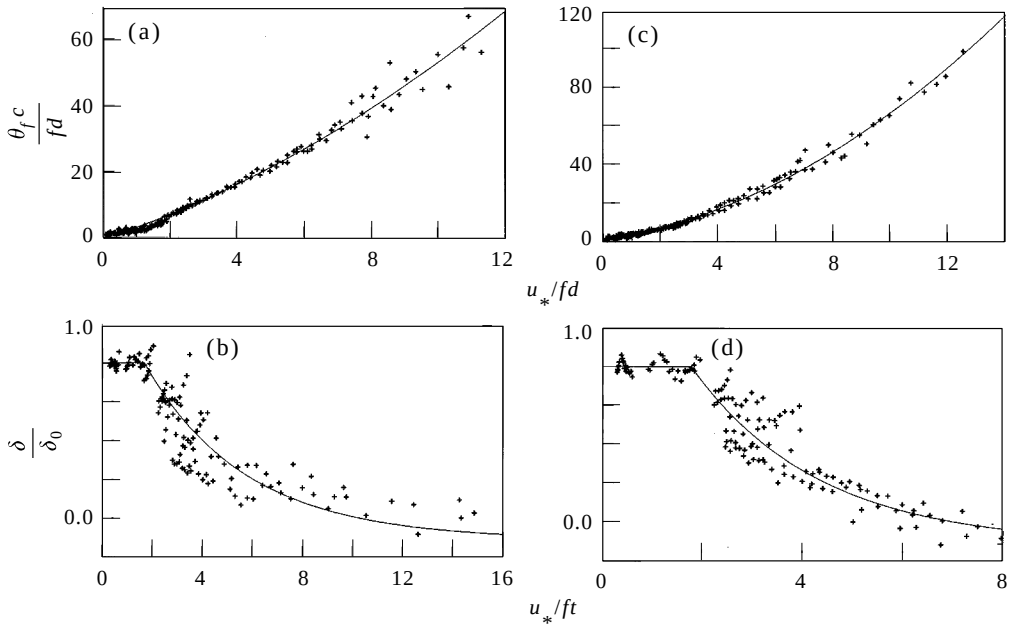

Figure 5. Acoustic impedance of louvres 2 and 3. +, experiment; ——, curve fitting formulae. Louvre 2: (a) resistance, (b) end correction. Louvre 3: (c) resistance, (d) end correction.

t/d and u_*/fd. For the resistance, second order polynomials were employed, having the form

$$\theta_f c/fd = A_1 + A_2(u_*/fd) + A_3(u_*/fd)^2, \tag{14}$$

where $A_1 \cdots A_3$ are constants given in Table 3.

The mass end correction is given by the expressions

$$\delta/\delta_0 = B_1 + B_4, \qquad u_*/ft \leqslant B_2/B_3,$$

$$\delta/\delta_0 = B_1 \exp\{B_2 - B_3 u_*/ft\} + B_4, \qquad u_*/ft > B_2/B_3, \tag{15}$$

where $B_1 \cdots B_3$ are constants given in Table 4.

TABLE 3

Curve fitting constants for the resistance of the louvres

Louvre	A_1	A_2	A_3
1	1·424	1·128	0·303
2	−0·528	3·359	0·202
3	0·670	2·351	0·432

TABLE 4

Curve fitting constant for the mass end correction of the louvres

Louvre	B_1	B_2	B_3	B_4
1	0·7	0·629	0·286	0·2
2	0·9	0·250	0·250	−0·1
3	0·9	0·707	0·400	−0·1

3.2. ACOUSTIC IMPEDANCE WITH A POROUS BACKING

The experimental method described previously for measuring the impedance without a porous backing material can also be applied to measurements with a porous medium on the side of the perforate remote from the flow. However, the normalized acoustic impedance must be re-defined to take account of the porous material, and accordingly equation (2) is now written in the form

$$z_o = z_a \frac{A_o}{A_c}\left[\frac{-\sin\phi + \mathrm{i}(R\cos k_a L - \cos\phi)}{R\sin k_a L}\right]. \tag{16}$$

The resistance and reactance are then found by taking, respectively, the real and imaginary parts of equation (16), since z_a and k_a are complex.

It is still possible to non-dimensionalize the resistance and mass end correction in the same manner as before, but the problem is complicated by the fact that z_a and k_a are complex and frequency dependent. When the orifice resistance, for example, was plotted against u_*/fd for a given value of u_*, it proved to be impossible to combine data measured for an individual perforate, with differing values of u_*, in a single plot in the manner employed in the previous section. Instead, the experimental data obtained here with a porous medium were plotted against frequency for each value of friction velocity. For the purposes of silencer design, however, it is highly desirable to be able to express the perforate impedance as a function of flow speed or friction velocity. Accordingly, a semi-empirical predictive model was developed, combining the formulae for the perforate impedance in the absence of a porous medium with the predicted bulk acoustic properties of the absorbent.

This prediction method for the perforate impedance in the presence of a porous medium is based on the heuristic assumption that the hydrodynamic effects of grazing flow on the orifice resistance and end correction on the side of the orifice facing the flow are unaltered by the presence of the porous medium, which has the principal effect of changing the mass end correction on the side of the orifice facing the porous material. For a single orifice with no porous backing and no mean flow present, the normalised mass end correction is given by [21]

$$\chi = 0{\cdot}425kd. \tag{17}$$

The equivalent mass end correction when a porous material is present is obtained [17] by substituting the properties of air for the properties of the porous medium, namely,

$$\chi_{abs} = 0{\cdot}425dz_a\Gamma/\rho c. \tag{18}$$

Note that the end correction is now complex, and has a resistive component. The perforate impedance is given in terms of the empirically-predicted impedance ζ from equations (7)–(15) as

$$z_o/\rho c = \zeta - \mathrm{i}0{\cdot}425kd + 0{\cdot}425dz_a\Gamma/\rho c, \tag{19}$$

where the mass reactance of equation (7) has been replaced by the complex value from equation (18). Values for the propagation constant and characteristic impedance of porous materials are well documented; see, for example, the empirical study by Delany and Bazley [22]. More recently Kirby and Cummings [23, 24] introduced a semi-empirical model, describing the bulk acoustic properties of a number of porous media over a wide frequency range and avoiding the "non-physical" predictions which can often occur at low frequencies when the Delany and Bazley empirical approach is used. The semi-empirical approach to predicting the bulk acoustic properties is adopted here and, in addition, the three fibrous porous materials studied in reference [24] are also included in the present investigation. These are "A glass", "E glass" and basalt wool.

Once values for the bulk acoustic properties have been obtained, equation (19) can be employed to predict the behaviour of the perforate with a porous backing.

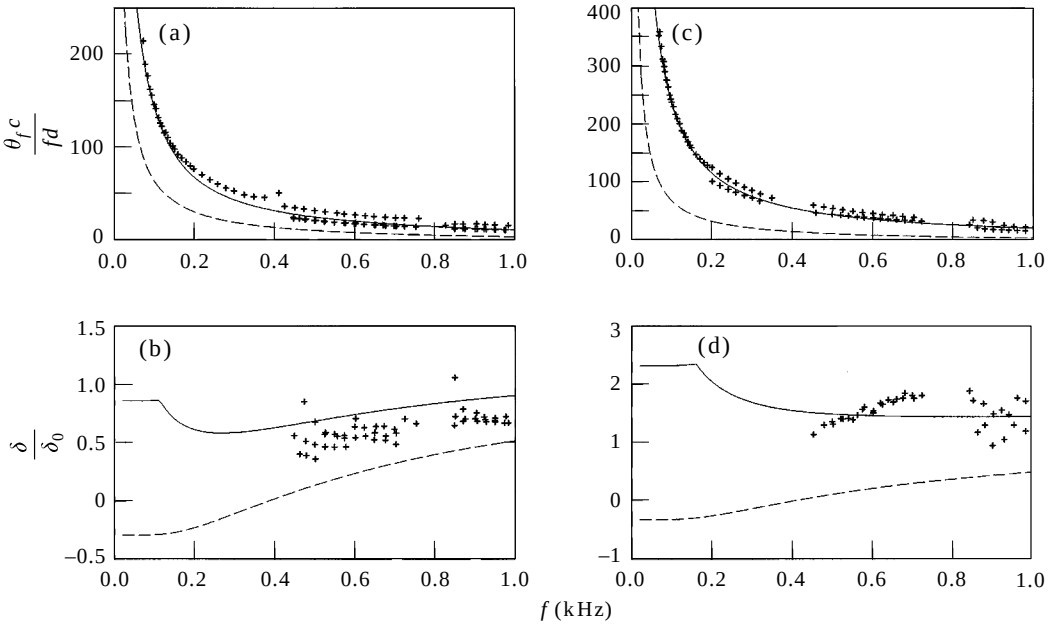

Figure 6. Acoustic impedance of perforates backed by a porous material. +, experiment; ——, semi-empirical predictions; ——, formulae for no absorbent backing. Plate 1, basalt wool, $u_* = 2{\cdot}2$ m/s: (a) resistance, (b) end correction. Plate 2, E glass, $u_* = 2{\cdot}2$ m/s: (c) resistance, (d) end correction.

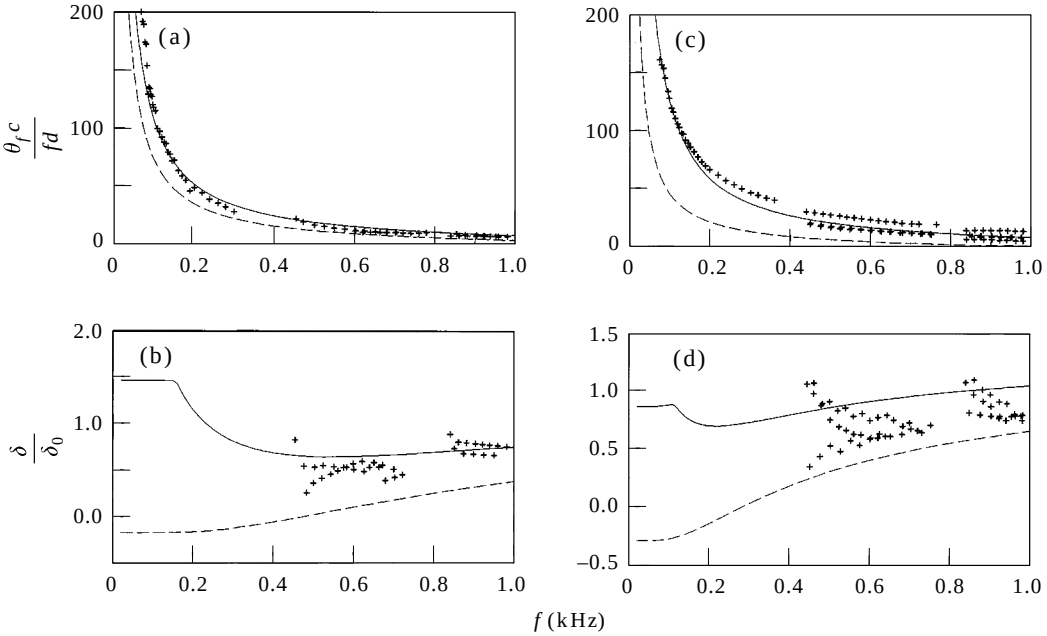

Figure 7. Acoustic impedance of perforates backed by a porous material. +, experiment; ——, semi-empirical predictions; – – –, formulae for no absorbent backing. Plate 3, A glass, $u_* = 2{\cdot}2$ m/s: (a) resistance, (b) end correction. Plate 1, basalt wool, $u_* = 1{\cdot}6$ m/s: (c) resistance, (d) end correction.

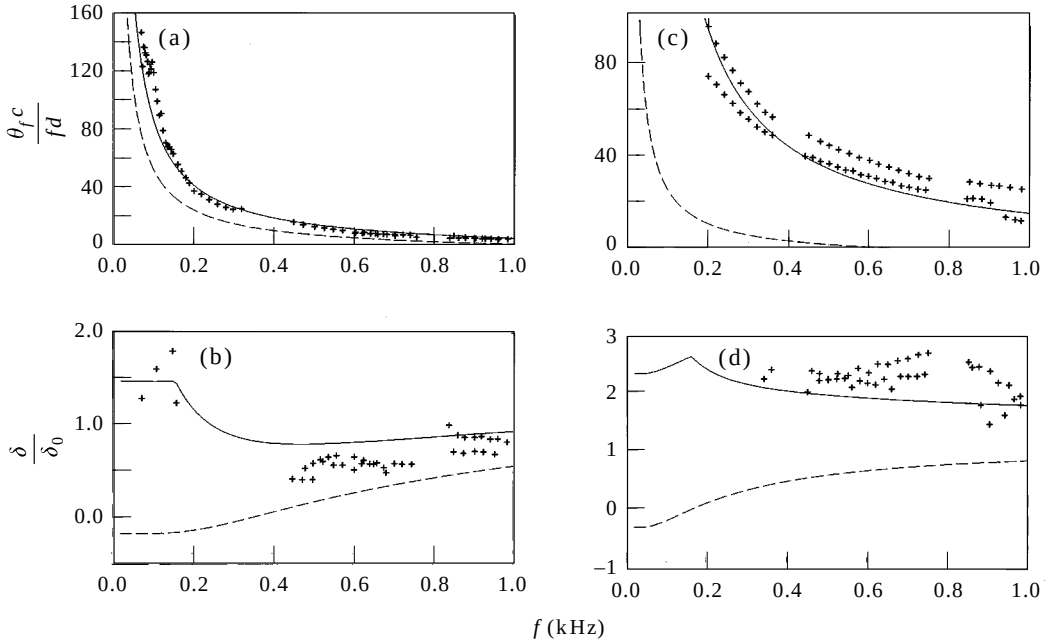

Figure 8. Acoustic impedance of perforates backed by a porous material. +, experiment; ——, semi-empirical predictions; – – –, formulae for no absorbent backing. Plate 3, A glass, $u_* = 1{\cdot}6$ m/s: (a) resistance, (b) end correction. Plate 2, E glass, $u_* = 0{\cdot}9$ m/s: (c) resistance, (d) end correction.

The accuracy of the semi-empirical predictions can be assessed by comparing them to measured data. In the case of perforates with a porous backing, we define θ_f and δ in terms of $z_o/\rho c$ in equation (19) as

$$\theta_f = \mathrm{Re}\,(z_o/\rho c) - \theta_{visc}, \qquad \delta = \mathrm{Im}\,(z_o \rho c)/k - t, \tag{20a, b}$$

with δ_0 being defined as before, in the *absence* of a porous medium. Now, both θ_f and δ include the effects of the porous medium as well as those of flow.

Experimental measurements were performed for both types of perforate and for the aforementioned three porous materials at three friction velocities: 0·986, 1·626 and 2·192 m/s. In Figures 6–8, experimental data are shown for plates 1 to 3 backed by various materials. (Some of the results are not shown here because of the large amount of data obtained.) The semi-empirical predictions (equation (19)) and the empirical formulae for the perforates without a porous backing (equations (12) and (13)) are also shown. The predictions with no absorbent present have been included in order to show the additional effect of the porous material.

Next, the louvred plates were measured with a porous backing, but no detectable difference between the results with and without the porous material was observed. The reasons for this will be discussed in the following section.

4. DISCUSSION OF RESULTS AND CONCLUSIONS

The experimental results obtained for the flat plates without a porous backing material will be discussed here first since these allow a straightforward comparison to be made with the data published by Goldman and Chung [12], Kooi and Sarin [13] and Cummings [14]. It is evident from Figures 3 and 4 that the data obtained without a porous material present agree qualitatively with other published data in that the resistances of the flat plates exhibit a linear relationship with u_*/fd, and for the mass end correction, decreasing values are observed as u_*/ft increases. A constant negative value for the mass end correction has been assumed at very high values of u_*/ft in accordance with the assumptions made by Cummings [14]. As expected, the spread of the resistance data is small; this is principally because the resistance can be measured with reasonable accuracy. The difficulties in measuring the mass end correction have been well documented and this is apparent in the large scatter of data present in Figures 3 and 4.

It can be seen from Figures 3(a–d) and 4(a, b) that the present end correction and resistance data differ significantly in detail from the empirical formulae of Cummings [14]. For plates 1, 2 and 3 the resistance measured here is greater than that predicted by Cummings while the end correction decreases with u_*/ft much less rapidly than is forecast by Cummings' formula. These discrepancies are greater than those noted by Cummings [14] between his data and those of Kooi and Sarin [13]. The reasons for these differences are not clear, but may be associated with the fact that the orifice length in the Cummings' experiments was at least twice that in the present investigation; there may also have been significant differences between the flow structures in the two sets of experiments. It does seem clear that neither Kooi and Sarin [13], Cummings [14] nor the authors have obtained universally applicable formulae for resistance and end correction. The three sets

of data should, perhaps, each be regarded as self-contained and applicable in different situations. For example, the Kooi and Sarin data would be applicable to jet engine inlet silencers, whereas the present data should be used in flow duct silencers embodying perforates similar to those investigated here.

Since the main objective of the present study was to examine the effects of a porous medium on the perforate impedance, it was not considered appropriate to investigate the question of the aforementioned discrepancies further. However, future efforts to combine the separate sets of data in single correlations—perhaps involving additional parameters—might prove fruitful.

It is worth noting that orifice interaction effects were negligible in the tests reported here. Fully perforated plates, those with 50% of the holes blocked and single orifices were tested but all the experimental data collapsed onto a single curve. It can therefore be concluded that measuring multi-holed perforates has not caused the differences in predictions between the present study and that of Cummings [14], and therefore single orifice data appear to be valid for predicting the impedance of multi-hole perforates providing one accounts for the area porosity of the perforate.

The experimental results obtained for the louvres without the presence of a porous material show qualitatively but not quantitatively the same behaviour as the flat plates. The most obvious difference is that the resistance curves for the louvres have a distinctly non-linear shape. A quadratic curve was found to fit the resistance data well for each louvre. The mass end correction of the louvres does not show such a pronounced decrease, for increasing values of u_*/ft, as that of the plates. Of course, as stated in section 3.1, δ/δ_0 does not equal 1 when $u_*/ft = 0$ because of the way in which the equivalent diameter of a louvred hole is defined. The reasons for the differing behaviour of both the resistance and the reactance in the cases of plates and louvres are not entirely clear. Two factors are the differing orifice geometry and the fact that, in the case of louvres, the orifice is orientated normal to the grazing flow. These are no doubt partly responsible for the differing behaviour of louvres and plates, although a detailed knowledge of the acoustic flow pattern through the louvre orifice would be necessary in order to pinpoint any physical mechanisms that would explain the differences. Louvres and plates show a similar degree of scatter in the experimental data, although the resistance data from louvres exhibit less scattering at lower values of u_*/fd. It was found to be impossible to express the measured data from louvres as a function of t/d, which is perhaps not surprising given the difference in geometrical shape between the louvres. Consequently the impedance must be measured experimentally for each louvre geometry.

Placing a porous material behind a flat perforate can be seen to cause a large increase in the impedance, which is dependent on the properties of the porous material. As one would expect, materials with a high flow resistivity—such as E glass—cause the largest increase in impedance. The resistance data exhibit a degree of scatter similar to that observed in the absence of a porous medium, but a high degree of scatter is observed in the mass end correction data and, moreover, data below 450 Hz were virtually unobtainable. It may also be seen from the plots on which the frequency is the abscissa that measurements were unobtainable around

400 and 800 Hz; this problem was probably caused by the presence of a pressure node in the test duct.

When measurements were carried out with the flat plates backed by porous materials it was apparent that the results were strongly dependent upon the density of the material immediately adjacent to the holes. This indicates that the porous material has only a very localized effect upon the orifice impedance. The results shown in Figures 6–8 were obtained by using a regular, flat layer of absorbing material covering the near field of each orifice. Indeed it can be seen in the resistance data presented here that, especially at low friction velocities, different trends in the data occur. The reason for this is that slight inhomogeneity of the material was inevitable, since the porous media were supplied in bulk form and were packed into the cavity by hand. This localized effect was particularly obvious when measurements were carried out on louvres backed by a porous material. The orientation of each louvre orifice prevents the porous medium lying flush with the end plane of the orifice. Because of this, it was found that the porous material had no measurable effect upon the acoustic impedance of the louvres. The localized effect of the absorbent has important consequences when the data measured here are used to predict the attenuation of mass-produced silencers. In commercial silencers the porous material is often randomly packed around the perforate tube, and therefore it can be expected that only a percentage of the material will lie in the near field of the perforations, even in the case of plain circular holes. This will inevitably lead to the formulae presented here over-predicting the impedance obtained in practice. Quantification of the variation in absorbent packing density would be necessary in order that a representative average orifice impedance could be found (see reference [25] for further discussion).

The semi-empirical predictions for the resistance of the flat perforates backed by porous material shown in Figures 6–8 (solid lines) are in good agreement with measured data. This is especially true at higher friction velocities where the resistance is higher and can therefore be measured more accurately. As before, there is considerable scatter in the measured end correction data. Figures 6–8 indicate that, in most cases, the end correction has been over-predicted. This may be partly because of limited measurement accuracy and partly because of some additional mechanism that reduces the effect of the absorbent on the mass end correction. A significant feature of the predictions is that at low frequencies an increase in the mass end correction is forecast, in contrast to the falling negative values measured in the absence of an absorbent. The lack of experimental data at low frequencies does not, however, allow any conclusions to be drawn concerning the validity of these predictions at low frequencies. The semi-empirical prediction scheme does, however, yield good agreement with experimental data for the resistance and appears to be at least adequate for the mass end correction. It is a useful method for estimating the additional effect of the porous material on the behaviour of a "flat" (i.e. non-louvred) perforate, and has the considerable advantage of only requiring data obtained from perforates without a porous backing. These can be expressed as a function of friction velocity and, especially for flat perforates, have been well documented both here and by other

authors [13, 14]. In addition, any porous material can be included, provided its propagation constant and characteristic impedance are known.

The principal effect of a porous medium on the impedance of a flat perforate is to introduce an additional complex component, as compared to plates without absorbent backing. The magnitude of this increase in impedance is such that, even for plates with a large percentage open area, the inclusion of perforates in the modelling of dissipative silencers is necessitated. This is of lesser importance when louvres are present since the porous material has no measurable effect upon their acoustic impedance, but they should still be included in design formulations for both dissipative and reactive silencers.

ACKNOWLEDGMENT

This work received financial support from the Department of Transport and an industrial consortium under LINK programme grant LAMPS2, "Computer Aided Design Methods for Vehicle Silencers", ref. TIO-50, 1992–95.

REFERENCES

1. D. Ronneberger 1972 *Journal of Sound and Vibration* **24**, 133–150. The acoustic impedance of holes in the wall of flow ducts.
2. K. J. Baumeister and E. J. Rice 1978 *American Institute of Aeronautics and Astronautics Journal* **16**, 233–236. Flow visualization in long-neck Helmholtz resonators with grazing flow.
3. P. A. Nelson, N. A. Halliwell and P. E. Doak 1981 *Journal of Sound and Vibration* **78**, 15–38. Fluid dynamics of a flow excited resonance, part I: experiment.
4. M. S. Howe 1979 *Journal of Sound and Vibration* **67**, 533–544. The influence of grazing flow on the acoustic impedance of a cylindrical wall cavity.
5. B. E. Walker and A. F. Charwat 1982 *Journal of the Acoustical Society of America* **72**, 550–555. Correlation of the effects of grazing flow on the impedance of Helmholtz resonators.
6. D. Ronneberger 1980 *Journal of Sound and Vibration* **71**, 565–581. The dynamics of shearing flow over a cavity—a visual study related to the acoustic impedance of small orifices.
7. S. Kaji, M. Hiramoto and T. Okazaki 1984 *Bulletin of the Japan Society of Mechanical Engineers* **27**, 2388–2396. Acoustic characteristics of orifice holes exposed to grazing flow.
8. A. S. Hersh, B. Walker and M. Bucka 1978 *American Institute of Aeronautics and Astronautics*, Paper 78-1124. Effect of grazing flow on the acoustic impedance of Helmholtz resonators consisting of single and clustered orifices.
9. K. Narayana Rao and M. L. Munjal 1986 *Journal of Sound and Vibration* **108**, 283–295. Experimental evaluation of impedance of perforate with grazing flow.
10. A. Goldman and R. L. Panton 1976 *Journal of the Acoustical Society of America* **60**, 1397–1404. Measurement of the acoustic impedance of an orifice under a turbulent boundary layer.
11. D. Coles 1956 *Journal of Fluid Mechanics* **1**, 191–226. The law of the wake in the turbulent boundary layer.
12. A. Goldman and C. H. Chung 1982 *Journal of the Acoustical Society of America* **71**, 573–579. Impedance of an orifice under a turbulent boundary layer with pressure gradient.

13. J. W. KOOI and S. L. SARIN 1981 *American Institute of Aeronautics and Astronautics*, Paper 81-1998. An experimental study of the acoustic impedance of Helmholtz resonator arrays under a turbulent boundary layer.
14. A. CUMMINGS 1986 *Acustica* **61**, 233–242. The effects of grazing turbulent pipe-flow on the impedance of an orifice.
15. U. INGARD 1953 *Journal of the Acoustical Society of America* **25**, 1037–1061. On the theory and design of acoustic resonators.
16. K. P. FLYNN and R. L. PANTON 1990 *Journal of the Acoustical Society of America* **87**, 1482–1488. The interaction of Helmholtz resonators in a row when excited by a turbulent boundary layer.
17. U. INGARD and R. H. BOLT 1951 *Journal of the Acoustical Society of America* **23**, 533–540. Absorption characteristics of acoustic material with perforated facings.
18. W. A. DAVERN 1977 *Applied Acoustics* **10**, 85–112. Perforated facing backed with porous materials as sound absorbers—an experimental study.
19. R. L. PANTON 1984 *Incompressible Flow*. New York: Wiley.
20. V. C. PATEL 1965 *Journal of Fluid Mechanics* **23**, 185–208. Calibration of the Preston tube and limitations on its use in pressure gradients.
21. J. W. STRUTT (Lord Rayleigh) 1896 *Theory of Sound* (Volume II). London: Macmillan.
22. M. E. DELANY and E. N. BAZLEY 1970 *Applied Acoustics* **3**, 105–116. Acoustic properties of fibrous media.
23. R. KIRBY and A. CUMMINGS 1995 *Proceedings of Euro-Noise* 95 **3**, 835–840. Bulk acoustic properties of rigid fibrous absorbent extended to low frequencies.
24. R. KIRBY and A. CUMMINGS 1997 *Applied Acoustics* (to appear). Prediction of the bulk acoustic properties of fibrous materials at low frequencies.
25. R. KIRBY 1996 *Ph.D. Thesis*, University of Hull. The acoustic modelling of dissipative elements in automotive exhausts.